1980

Near bottom speed and temperature observations on the Blake-Bahama outer ridge

Georges L. Weatherly

Mark Wimbush
University of Rhode Island, mwimbush@uri.edu

Citation/Publisher Attribution
Weatherly, G. L., and Wimbush, M. (1980), Near-bottom speed and temperature observations on the Blake-Bahama Outer Ridge, *J. Geophys. Res.*, 85(C7), 3971– 3981, doi: 10.1029/JC085iC07p03971. Available at: https://doi.org/10.1029/JC085iC07p03971

Near bottom speed and temperature observations on the Blake-Bahama outer ridge

JOURNAL OF GEOPHYSICAL RESEARCH, VOL. 85, NO. C7, PAGES 3971-3981, JULY 20, 1980

Near-Bottom Speed and Temperature Observations on the Blake-Bahama Outer Ridge

GEORGES L. WEATHERLY

Department of Oceanography and Geophysical Fluid, Dynamics Institute
Florida State University, Tallahassee, Florida 32306

MARK WIMBUSH

Graduate School of Oceanography, University of Rhode Island, Kingston, Rhode Island 02881

Speed and temperature measurement made in the bottom boundary layer (BBL) in the region of the Western Boundary Undercurrent at 28°22'N, 74°13'W over an ~11 day period are presented. The observations suggest that the BBL structure is consistent with that of a turbulent Ekman layer formed in an initially stably stratified fluid over a uniform surface even though they were obtained in and above an abyssal furrow. The inferred friction velocities u_* ($\bar{u}_* = 0.66$ cm/s) generally are larger than those inferred by Weatherly (1972) under the Florida Current and at times sufficiently large to result in erosion of some of the finer cohesive sediments if the criterion for their erosion summarized in McCave (1978) is assumed to apply at the site of the observations.

1. INTRODUCTION

Hollister et al. [1974] reported on an investigation to determine the type of topographic features responsible for hyperbolic traces seen in bottom fathometer records in the vicinity of the Blake-Bahama Outer Ridge (Figure 1). The features responsible for the hyperbolic echoes were found to be furrows in the ocean floor. The furrows in this area are described in detail by *Flood* [1978], and the following description is taken from this work. These remarkable features are long grooves in the ocean bottom of width 1–100 m, depth 0.5–20 m, and average spacing of about 50 m. They are aligned approximately parallel to measured bottom currents and sometimes join in tuning fork junctions which tend to open into the current flow. While furrows cover a wide range of sizes, they change slowly along a given furrow. Figure 2 is a photograph of a furrow in this area. This furrow, like other smaller ones observed in the area, has a flat bottom which meets the furrow walls at an angle of about 45°. The walls are upward-convex in profile and usually manifest ripples with typical wavelength 20 cm, height 5 cm, and orientation 45° to the furrow. Seen from above, the ripples on the two sides appear as arrowheads pointing in the downstream direction. Abyssal furrows are not unique to the Blake-Bahama Outer Ridge (BBOR) area [*Flood*, 1978]; they are best documented in this area.

The purpose of this paper is to report some near-bottom current measurements made in the furrowed region of the BBOR. The objective of the observations was to obtain data from which the bottom shear stress τ_0, or more specifically the friction velocity $u_* \equiv (\tau_0/\rho)^{1/2}$, where ρ is the water density, could be inferred to compare these with values thought to be necessary for the erosion of cohesive marine sediments. This information was sought to help assess whether these furrows are relic or active features.

The manner in which the friction velocity u_* was inferred from near-bottom current measurements is straightforward. The current speeds were measured at sufficient heights above bottom to delineate the logarithmic layer, that is, that region in which the mean current $U(z)$ varies logarithmically with height z above the bottom, namely,

$$U(z) = (u_*/\kappa) \ln z/z_0 \tag{1}$$

where κ is von Karman's constant and z_0 is the roughness parameter. With $U(z)$ measured at two or more different heights in the logarithmic layer and von Karman's constant known, u_* (and z_0) can be inferred by using (1). The confidence one has in the u_* values inferred in this manner depends on at least three factors.

The first factor is the accuracy of (1) as a representation for $U(z)$ near the bottom. The furrows, being oriented downcurrent and spaced about two boundary layer thicknesses apart, may be due to Langmuir-like circulation patterns or 'vortex rolls' in the bottom boundary layer (BBL). Such vortex rolls are thought to be ubiquitous features of turbulent stream flows including turbulent Ekman layers [*Tennekes*, 1973]. Regions of horizontal convergence (divergence) near the surface owing to these secondary circulations are regions of enhanced (reduced) turbulence production [*Tennekes*, 1973]. Thus the presence of secondary circulation patterns may not conflict with the flow being logarithmic near the surface. Logarithmic layers are observed near the surface in nearly all turbulent shear flows. However, whether a logarithmic layer can be expected to form over a longitudinally furrowed surface is not clear. This study indicates that, at least in the smaller furrowed region, this does happen. It appears that locally the BBL settles smoothly into the furrow in such a way that the local velocity profile is everywhere like that of a turbulent Ekman layer over a uniform surface.

The second factor hinges on the value of von Karman's constant κ used in (1) to evaluate u_*. As was discussed in *Tennekes and Lumley* [1972], κ is a constant only in the limiting sense of the turbulent Reynolds number $Re_* \equiv u_* h/\nu \to \infty$, where h is the boundary layer thickness and ν is kinematic viscosity. In the large Re_* encountered in the atmospheric layer there is some reason to believe that $\kappa = 0.35$ rather than the traditional value of 0.4 deduced from laboratory studies done at lower Re_* [*Businger et al.*, 1971). Since Re_* in this study is about 2 orders of magnitude smaller than that of the atmo-

Paper number 80C0238.
0148-0227/80/080C-0238$01.00

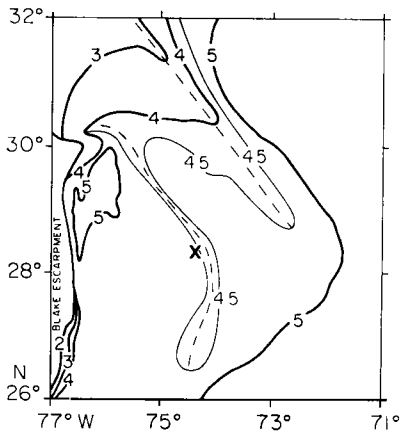

Fig. 1. Sketch of bathymetry in the Blake-Bahama Outer Ridge area inferred from *Flood* [1978, Figure 2.1]. Numbers are depths in kilometers. The two ridge crests are indicated by dashed lines and the site of the measurements by a cross.

spheric boundary layer, we take $\kappa = 0.4$. If indeed the value of 0.35 as was suggested by *Businger et al.* [1971] is appropriate for the present data set, the u_* values presented here are overestimated by about 14%. A second uncertainty in choosing a value of κ arises when the fluid is no longer clean but is sediment laden. Large concentrations of sediment in water lead to an apparent reduction in κ by as much as 50% [*Yalin*, 1977]. However, because of the low u_* values inferred in this study, in comparison with those in *Smith and McLean* [1977], the suspended sediment concentration gradients are thought to be sufficiently small not to affect κ and hence the speed profile. The third factor is the statistical adequacy of the data on which the u_* calculations are based. This is determined by the accuracy of the rotors as current sensors, the averaging process by which the current speed averages $U(z)$ are formed, and the number of levels z within the logarithmic layer at which rotors providing usable data are positioned. The accuracy of the rotors is discussed in section 3*b*. The averaging process is discussed in section 3*c*. The number of usable rotor levels

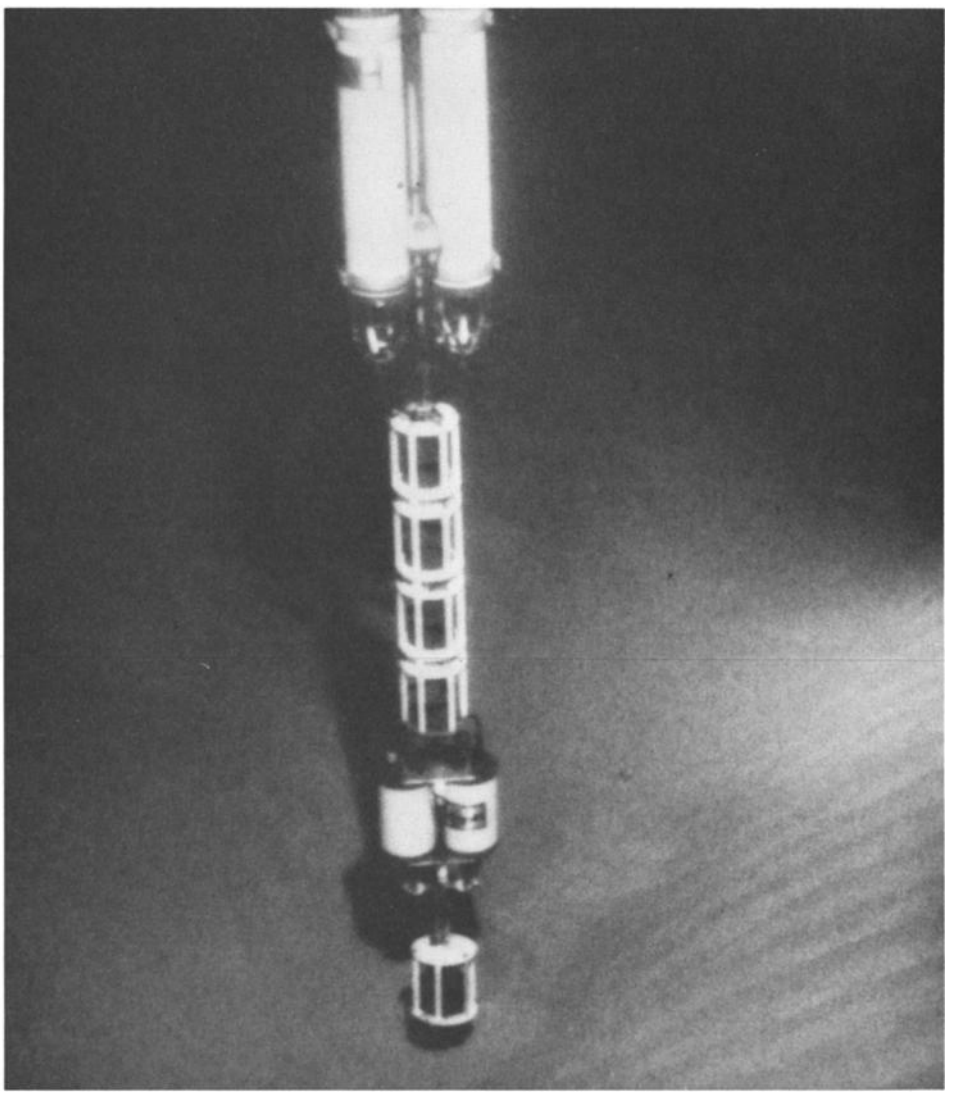

Fig. 2. Photograph of the furrow in which the profiling instrument (Figure 3) landed. The anchor weight indicated in Figure 3 is buried beneath the furrow floor. For reference the dimensions of the lowest rotor cage are 23 cm × 21 cm.

within the logarithmic layer was six, which is considerably greater than the required minimum of two. So far as these statistical considerations are concerned, we feel that the u_* values have a standard error of about 0.5 cm/s.

2. EXPERIMENT

The site of the observations, 28°22'N, 74°13'W, is on the western flank of one of the two ridges which comprise the BBOR (Figure 1) in water of depth 4750 m. The Western Boundary Undercurrent supposedly flows along isobaths northward at this site; further downstream it is believed to be deflected counterclockwise still following isobaths and to flow southward at the base of the Blake Escarpment [*Heezen and Hollister*, 1971]. Furrows are nearly ubiquitous features in the BBOR area, being absent only on the crests of the two ridges [*Flood*, 1978]. The site is about 11 km downslope (west) of the Bahama Outer Ridge crest and about an equal distance upslope from the eastern edge of a region of large abyssal mud waves (amplitudes tens of meters and wave lengths about 2 km) [*Flood*, 1978]. The sediments in this area are cohesive muds of composition 2–11% sand, 31–36% silt, and 58–63% clay [*Flood*, 1978].

The instrument used to measure the speed profile is shown schematically in Figure 3. It is very similar to an instrument described by *Weatherly* [1972], which was used to measure the speed profile in the bottom boundary layer of the Florida Current. It is a different instrument, however, not previously described, and a brief description follows. On the instrument are ten Savonious rotors and four thermistors. The height above bottom, during the experiment, of each sensor's midpoint is given in Table 1. In a central pressure case the rotor revolutions are counted and displayed, at fixed preselected intervals, together with the thermistor temperatures and the time and date, on LED displays which are photographed with a shutterless 16 mm camera. Approximately 7000 exposures can be made on one 30 m roll of film. The sampling interval can be varied in increments of 1 min from 3–100 min. For this experiment the sampling time was 9 min. The temperature that is recorded in each frame is the average temperature for the first minute following the previous frame. A cast lead anchor weight is released when either of the two acoustic releases is fired. The releases were modified by the manufacturer, so the release mechanism for each is remote from the release electronics (acoustic release in Figure 3).

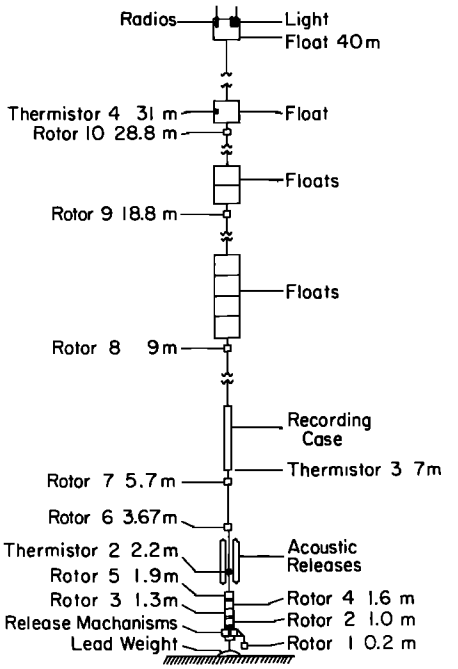

Fig. 3. Schematic of the profiling instrument. The lowest part of this instrument appears in Figure 2.

The instrument was launched on September 18, 1977, and reached the bottom at about 0300 UT on September 19, 1977. It was inspected by the submersible *Trieste II* on September 24, 1977. Figure 2, one of those photographs taken during that inspection, shows that it landed at the center of the floor of a smaller furrow and that the anchor weight had sunk about 20 cm into the furrow floor. Our intent was to have the *Trieste II* position the instrument between two furrows if it fell in or near a furrow. However, because of an inoperative mechani-

TABLE 1. Heights of Various Sensors Above the Seabed With Mean Parameters Recorded and Associated Time Scales

	Rotor Height, m	Average Speed, cm/s	T (Equation (2)), min	z/u_*, min	Thermistor	Thermistor Height, m	Average Temperature, °C
Rotor							
1	0.18 ± 0.01	6.00	33	0.4	1	0.90	2.05
2	1.05 ± 0.01	8.83	62	2.7	2	1.35	2.15
3	1.33 ± 0.01	9.32	67	3.4	3	5.77	2.17
4	1.62 ± 0.01	(10.21)	(67)	4.1	4	29.7	(2.12)
5	1.89 ± 0.01	9.94	76	4.8			
6	3.67 ± 0.02	10.98	111	9.3			
7	5.65 ± 0.02	11.70	143	14.3			
8	9.00 ± 0.10	(14.03)	(123)	22.7			
9	18.75 ± 0.15	14.59	243	47.3			
10	29.29 ± 0.20	(14.06)	421	74.0			
Tripod	0.70 ± 0.05	10.5*				1.0	2.19

The value of u_* used in forming the time intervals T (see (2)) and z/u_* is 0.66 cm/s. Suspect values are given in parentheses. Current averages are over the period September 19 0300 UT to September 29 1910 UT. Temperature averages begin September 19 1200 UT to exclude initial stabilizing period.

*Average direction at 0.94 m height is 329°T.

cal arm on the *Trieste II*, no such maneuver was attempted. The instrument left the bottom on acoustic command at 1911 UT on September 29, 1977.

A second instrument deployed in the area consists of a tripod frame, in which is mounted a camera system to take time sequences of bottom photographs, and a single vector averaging current meter (VACM), to record the current speed and direction at elevations of 70 and 92 cm, respectively. A similar apparatus is described in *Wimbush and Lesht* [1979].

This tripod instrument was launched on September 18, 1977, and reached the bottom at about 0130 UT on September 19. It was found by *Trieste II* on September 24 a few meters from the edge of a furrow and about 800 m east of the other instrument. (Only our dislike of being thought ridiculous prevents us from suggesting that horizontal convergence owing to furrow-associated vortex rolls in the BBL was responsible for one instrument landing directly in a furrow and the other landing a few meters from a furrow rim.) The submersible then maneuvered the tripod to the rim of the furrow so that the camera was looking at the ripples in the upper part of the furrow wall. Figure 4 is a photograph taken just after the instrument has been repositioned. At the end of the experiment the release system failed, and the instrument was lifted off the bottom by *Trieste II* at 2305 UT October 1, 1977.

A total of three dives were made by the submersible *Trieste II* in the vicinity of these instruments. The information on the sediment given earlier was deduced from bottom cores taken on one of those dives [*Flood*, 1978].

3. Results

a. *The Near-Bottom Current*

Since simultaneous measurements of currents at various heights in the benthic boundary layer are not yet common, it may be of interest to consider the speed time series obtained. Figure 5 is a time series plot of the 10, 9-min averaged, speeds obtained with the profile instrument during this experiment. Some features are noteworthy.

The currents near the bottom are more noisy than those, say, at 20 and 30 m above the bottom. The source of this noise is probably the shear generated turbulence in the BBL. In the equation for the turbulent kinetic energy [e.g., *Tennekes and Lumley*, 1972, equation (3.2.1)] the mean shear production term for the case of a horizontal mean current, $\hat{\imath}U(z)$, is $-\overline{uw}\,\partial U/\partial z$, where $\hat{\imath}u + \hat{\jmath}v + \hat{k}w$ is the turbulent velocity fluctuation, $\hat{\imath}$ and $\hat{\jmath}$ are horizontal and $\hat{k}$ vertical unit vectors, respectively, and the overbar denotes a Reynolds average, Since the Reynolds stress $-\overline{uw}$ is largest in the lowest part of the BBL as well as the mean vertical shear $\partial U/\partial z$, the level of shear-generated turbulence is expected to be largest in the lower part of

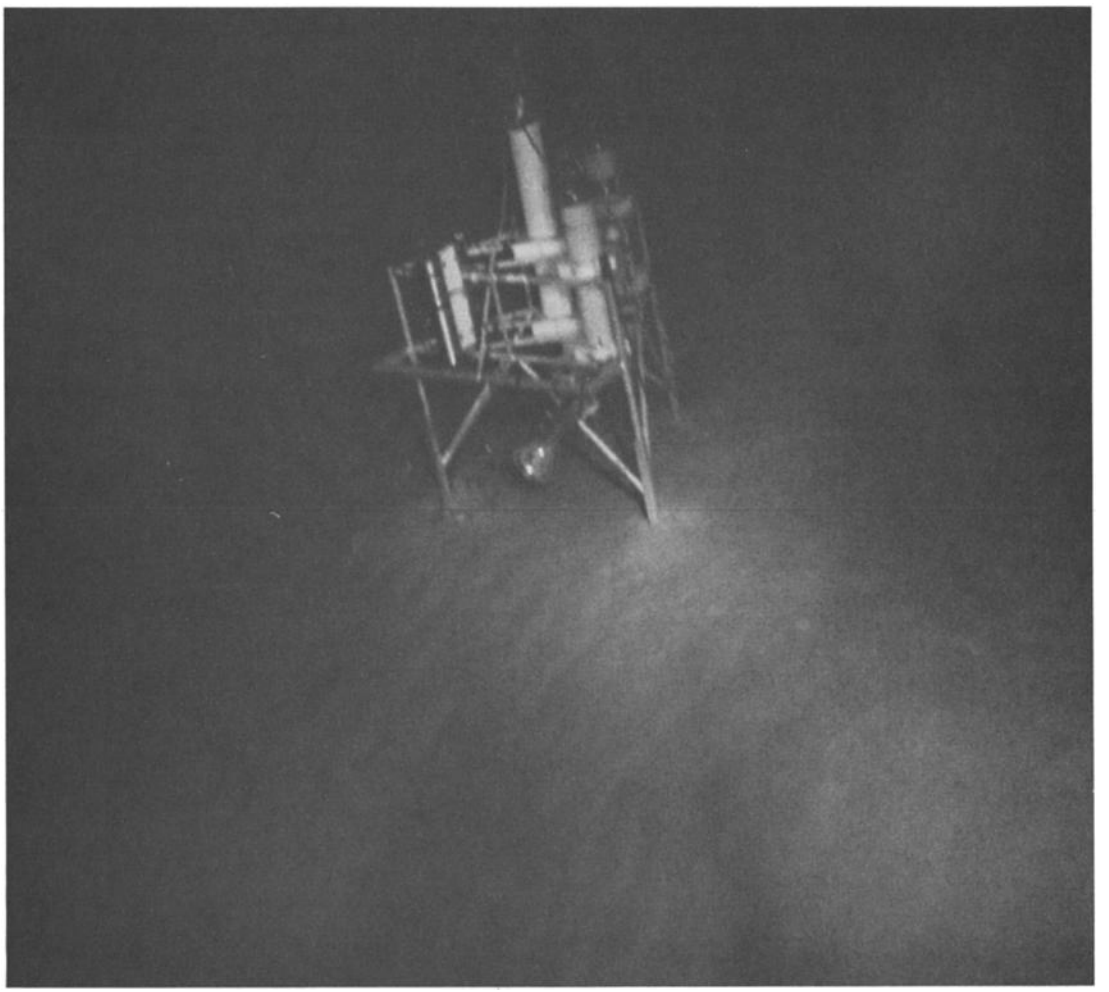

Fig. 4. Photograph of the tripod instrument after repositioning by *Trieste II* on a furrow flank. The length of one side of the tripod is 1.6 m.

the BBL. It is interesting to note that unlike the observations of *Wimbush and Munk* [1970] in the BBL in the eastern North Pacific and *Weatherly* [1972] in the BBL of the Florida Current, the noise level does not tend to increase when the mean current is decelerating, but here the rate of current change is much less. Indeed from Figure 5 it is apparent that the mean (over several hours) current at all levels is remarkably steady. Semidiurnal tidal and diurnal tidal-/inertial-type oscillations occur at all levels. (Inertial period at the latitude of the observations is 24.9 hours.) However, the amplitude of these oscillations is generally smaller in relation to the local mean current near the bottom, and the mean current is more steady there. One might suppose that this is due to constraints imposed by the furrow. However, *Weatherly and Van Leer* [1977] noted a similar behavior in the BBL on the continental shelf west of Florida, in a supposedly nonfurrowed area. Histograms of the speeds nearer the bottom tend to become bimodal as the height from the bottom increases (Figure 6).

The VACM record from the tripod instrument is shown in Figure 7. The disturbance early on September 24 is the repositioning by *Trieste II*. The mean velocity vector during the 5 days before and the 8 days after repositioning are (11.0 cm/s, 329°*T*) and (10.2 cm/s, 330°*T*), respectively. The mean directions are parallel to the furrow axis.

b. Quality of the Speed Data

The speed-measuring characteristics of the VACM used in the tripod instrument are discussed by *McCullogh* [1975]. Above the 2 cm/s rotor stall speed the rms error is about 0.3 cm/s in steady flows. The rotors used in the profile instrument are similar so that we could expect similar rms errors for them.

In a cursory look at Figure 5 speed records, one sees that the adjacent records look qualitatively similar, suggesting good data. However, three of the speed records in this figure are suspect. On recovery, faults were discovered in rotors 4, 8, and 10. A bearing on rotor 10 had backed down on the pivot, causing this rotor to turn less freely than the others. Table 1

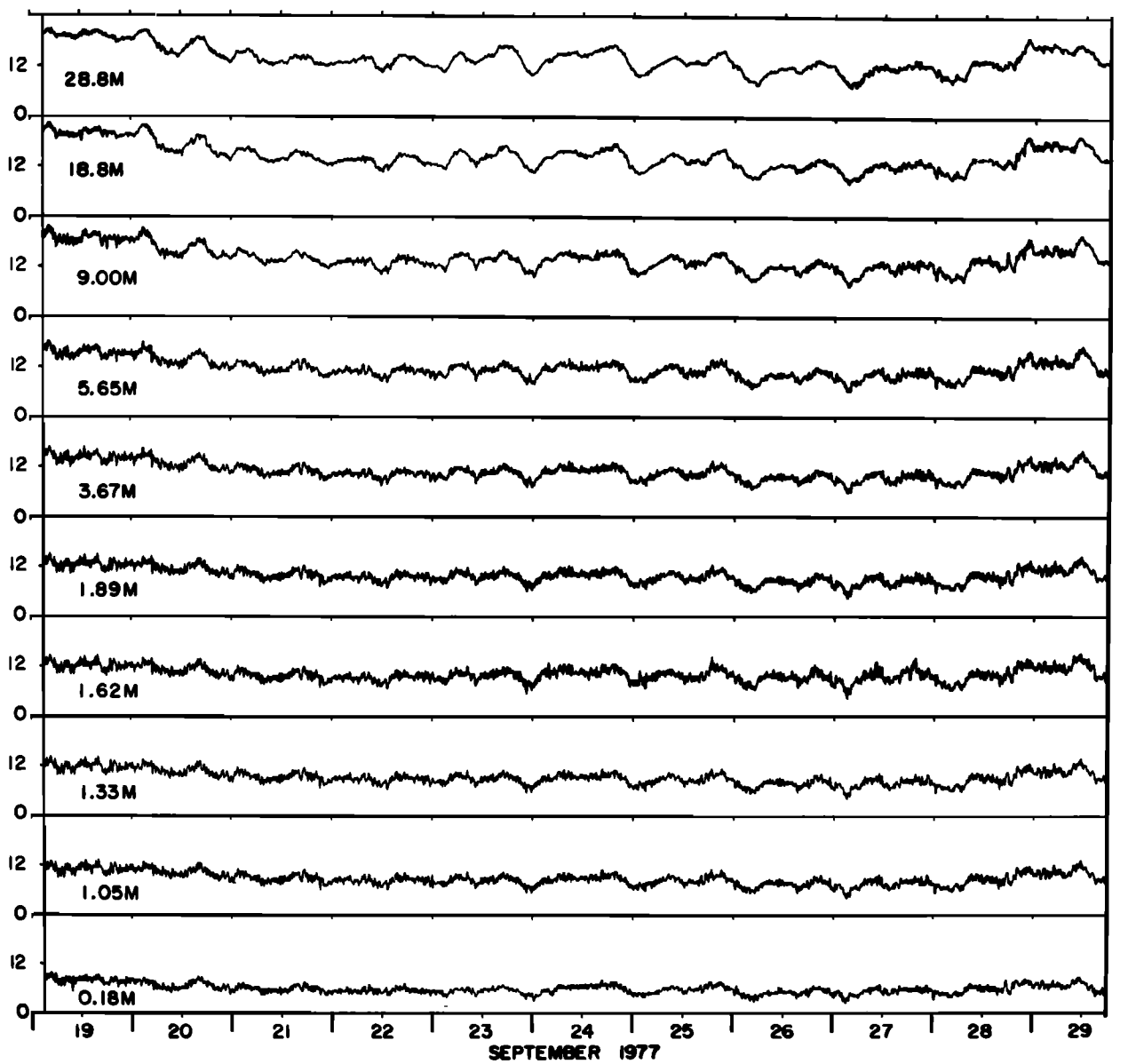

Fig. 5. Time series plot of the ten 9-min averaged speed records obtained from the profiling instrument.

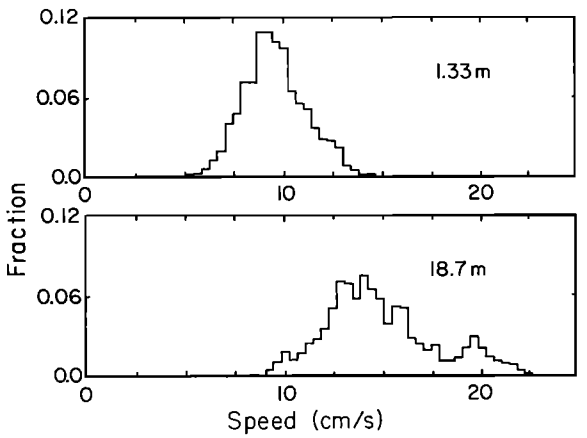

Fig. 6. Histograms of the 9-min averaged speed records at 1.33 and 18.7 m.

gives the mean speed over the experiment for each rotor. (Hereafter, unless otherwise stated, 'mean' denotes an average over the ~11 day period during which the profile instrument was on the sea floor.) It is seen that the speed for rotor 10 is somewhat less than that for the rotor immediately below it. The remaining nine average speeds are plotted as a function of height above the furrow floor in Figure 8*a*. In this figure the speeds of rotors 4 and 8, at $z = 1.62$ and 9.0 m, respectively, fall to the right of the smooth curve drawn through the remaining points. The speeds at these two levels appear to be overestimated. The mean speeds inferred at these two levels from the smooth curve in Figure 8*a* are indicated as solid circles in Figure 8*b*. In rotors 4 and 8 the reed switches which sense the rotor revolutions were found to have high contact resistance and, in the case of rotor 4, intermittent double contact closure.

c. *Time Averaging*

In (1) the speed U is an average speed. For the atmospheric boundary layer it has been found that the appropriate averaging interval is about 15–20 min. *Monin* [1970] justifies the use of this interval on the basis of a deep minimum in the spectrum at this point. *Wyngaard* [1973] estimates that for ($a \times 100$)% accuracy the averaging interval T should be

$$T \approx 2\,\tau_i\,\overline{u^2}/(U^2\,a^2) \tag{2}$$

where τ_i is the integral time scale which he approximates by z/U. For 1% accuracy in the atmospheric logarithmic layer, he estimates $T \approx 15$ min.

No comparable minimum has been noted for spectra obtained in the bottom boundary layer. However, this may be due to the spectral density $E(n)$, where n is frequency, being examined [*Wimbush and Munk*, 1970; *Weatherly*, 1972] rather than $nE(n)$. With a logarithmic frequency axis, the area under a plot of $nE(n)$ is proportional to the fluctuation energy. Figure 9*a* shows the spectrum $nE(n)$ of the speed record obtained at $z = 19$ m. Although this rotor was probably in the BBL (later we estimate the BBL thickness at about 30 m) this spectrum probably resembles one which would result from a record obtained above the BBL since the shear generated turbulence is greatly reduced at this level (Figure 5). For $n \gtrsim 0.1$ cph, this spectrum is approximately flat. A comparable spectrum for the rotor at $z = 1$ m, Figure 9*b*, is approximately flat for 0.1 cph $\lesssim n \lesssim$ 0.6 cph; but for $n \gtrsim 0.6$ cph, the energy level begins to increase and continues to increase until the Nyquist frequency is reached. Thus the region 0.1 cph $\lesssim n \lesssim$ 0.6 cph lying between the semidiurnal peak ($n = 0.0833$ cph) and the

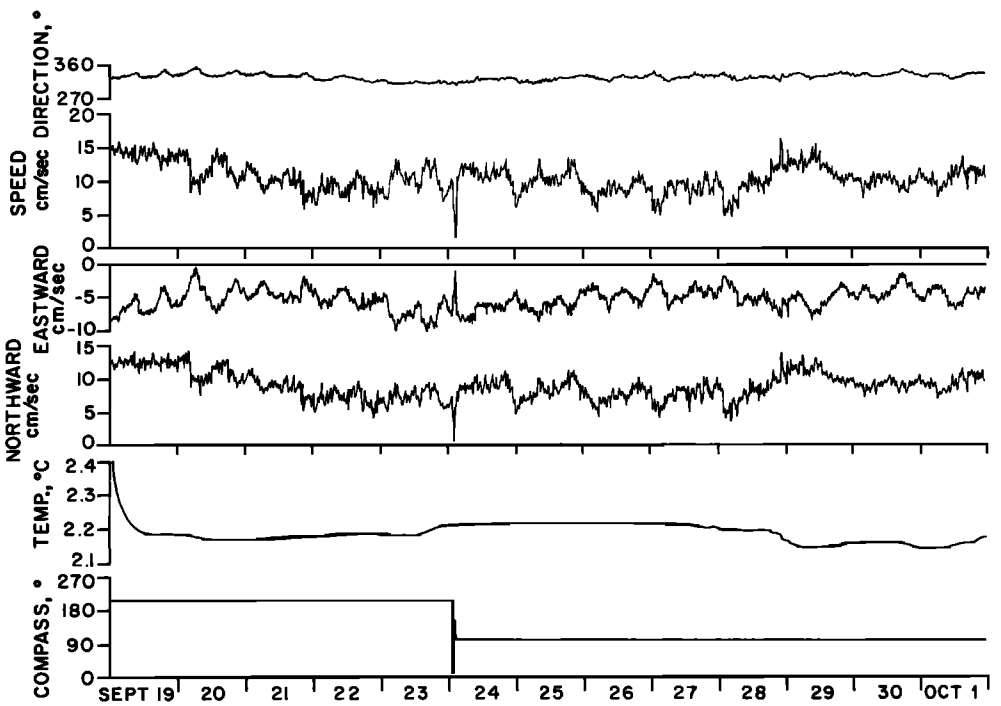

Fig. 7. Time series of the VACM record from the tripod instrument. Shown are current direction (in °T), speed, eastward and northward components, temperature, and compass heading. The temperature measuring circuit apparently took about 12 hours to stabilize at the beginning. The disturbance in compass heading, early September 24, is due to repositioning by *Trieste II*.

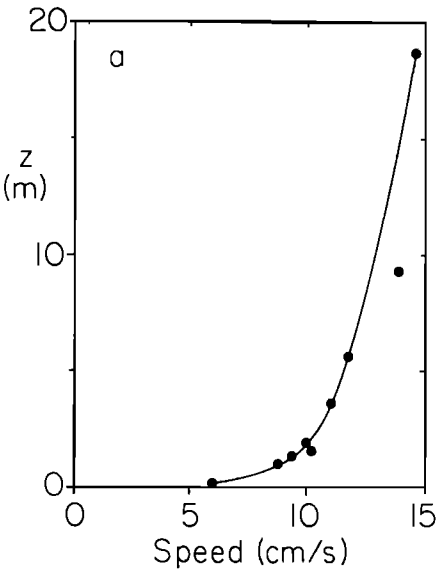

Fig. 8*a*

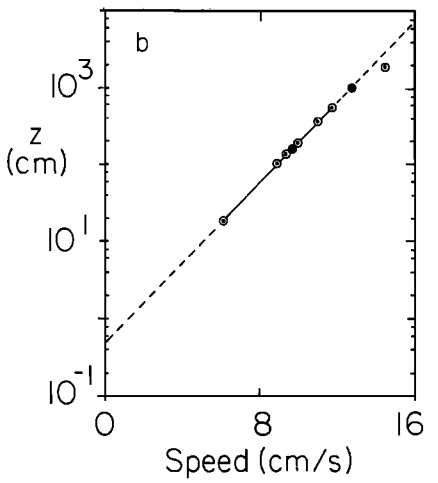

Fig. 8*b*

Fig. 8. (*a*) Mean (over the ~11 day period of observations) speed profile. The two values which lie off the curve are thought to be overestimated (see text). (*b*) Mean speed as a function of logarithm of height z above the furrow floor. The two values which fall off the smooth curve in Figure 8*a* are omitted; however, values read off the curve in Figure 8*a* for these two levels are indicated by solid circles.

broad rise beginning at $n = 0.6$ cph, can be considered as a shallow spectral valley or minimum. Following *Monin* [1970] the averaging interval should then lie between 1.7 and 10 hours. Values of T computed from (2) with $a = 0.01$ for the different rotor levels taking $\overline{u^2}/u_*^2 = \text{constant} \equiv A$ (valid only in the logarithmic layer) and $A = 2.78$ [*Mellor*, 1973] with $u_* = 0.66$ cm/s are listed in Table 1. For example, at $z = 5.65$ m, $T \approx 2.4$ hours. (As is discussed later, the logarithmic layer was thought to extend to $z = 5.65$ m). In summary, these arguments suggest that the averaging interval T should be between about 2 and 10 hours, (i.e., 2 hours $\lesssim T \lesssim$ 10 hours). This is appreciably longer than z/u_*, an averaging interval used in other studies [*Wimbush and Munk*, 1970; *Weatherly*, 1972]. In this study, various time-averaging intervals ranging from 9 min to about 10 days are considered.

d. Quality of Direction Data

No satisfactory study of the directional accuracy of the VACM has been carried out. In particular, one would like to know what would be the effect of a tilt of 15°, which is the approximate tilt of the VACM after positioning on the furrow flank (Figure 4). The vane is designed to have nominally neutral buoyancy in seawater, and it is felt that the 5–15 cm/s currents encountered here, the total standard error would be comparable to the compass and vane resolution of 2.8°.

e. Quality of the Temperature Data

The profile instrument used commercially produced temperature measuring electronics (model 37, Sea Data Corporation, Newton, Massachusetts). The manufacturer claims an absolute accuracy of 0.01°C and a resolution of several millidegrees. The record obtained from thermistor four at 30 m displayed a linear trend of about −0.4°C/11 days. This trend, thought to result from an electrical connector damaged during launch, was removed before computing the value given in Table 1 and plotting the values shown in Figure 13.

Accuracy and resolution of temperature recorded by the VACM is the same as for the profiling instrument.

f. Friction Velocity u_* and Roughness Parameter z_0

Because the profile instrument was located in a furrow, a priori we might expect the flow profile to differ from the logarithmic from within a distance above the furrow comparable to its width (≈0.5 m at the base and several meters at the top). However, this smaller furrow is not a trench with vertical walls. The sloping walls do have curvature and appear to meet the flat area outside the furrow smoothly or at a small angle (Figure 2). For smaller furrows the BBL may conform to or 'settle into' these furrows sufficiently smoothly that the local vertical structure is like that of a planetary boundary layer formed over a flat plane (i.e., a logarithmic layer overlain by a turbulent Ekman layer). The data presented here are consis-

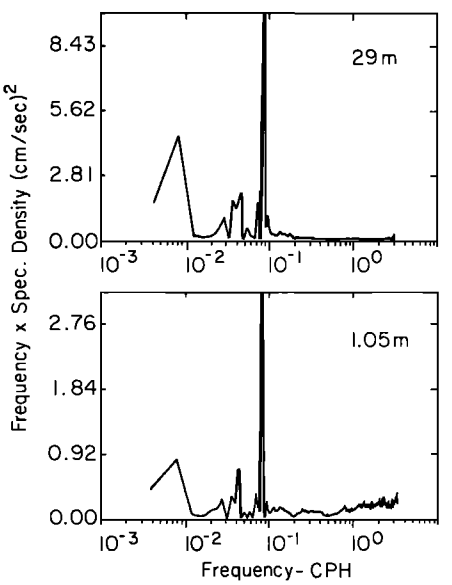

Fig. 9. Energy conserving spectra of speed records at (top) $z = 29$ m and (bottom) $z = 1.05$ m. Note that vertical scale is expanded in lower figure. Spectral estimates for frequencies >0.1 cph have been smoothed over 20 bands.

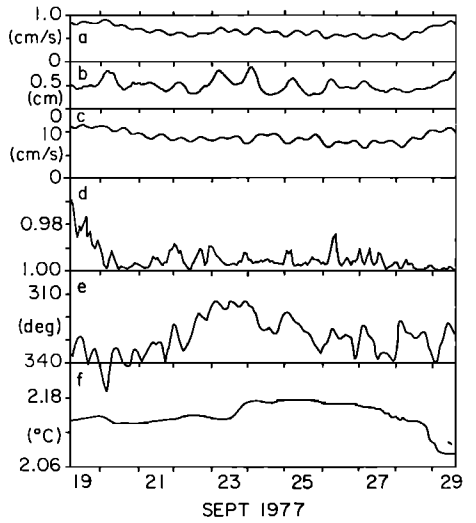

Fig. 10. (*a*) Time series plots of u_*, (*b*) z_0, and (*d*) r^2 determined from six-point (z = 0.18, 1.05, 1.33, 1.89, 3.67, and 5.65 m) least square fits of 6-hour averaged speeds to (1), (*c*) 6-hour averaged speeds at z = 1.05 m, (*e*) hourly averaged current direction near the rim in a neighboring furrow, and (*f*) 1.5-h averaged temperature at 1.35 m.

tent with this speculation about the vertical structure of the BBL in the area.

Figure 8*b* indicates that the mean speed profile was logarithmic for 0.18 m $\leq z \leq$ 5.65 m. The straight line in this figure is the least squares fit of (1) throught the lowest six points. The computed coefficient of determination r^2 (r is the correlation coefficient) of the data about this least squares fit is 0.9995. For a 0.99 confidence level in a six-point fit, the t test requires that $r^2 \geq 0.84$. This test reinforces what is suggested by a visual examination of Figure 8, namely, that (1) is a very good approximation to the mean speed data over the range 0.18 m $\leq z \leq$ 5.65 m. The u_* and z_0 values determined from this least square fit are 0.66 cm/s and 0.49 cm, respectively.

In section 3*c* the appropriate averaging interval is estimated to be of the order of several hours. In Figure 10 are shown time series of u_*, z_0, and r^2 determined from 6-hour averaged speeds. The input data are the six 6-hour averaged and decimated time series obtained from the rotors at z = 0.18, 1.05, 1.33, 1.89, 3.67, and 5.65 m. As is noted above, the 0.99 confidence level for a 6-point fit is that $r^2 \geq 0.84$. All the computed r^2 were greater than 0.84 (Figure 10*d*). One might conclude that all the 6-hour averaged profiles were logarithmic up to z = 5.65 m. However, as we try to demonstrate below, one must be careful in making conclusions from such a test.

In part from examination of sample profiles and the mean-speed profile (Figure 8*b*), we conclude that the flow was logarithmic up to about 6 m above the furrow bottom but never up to 19 m. The observed speed at 19 m (more precisely 18.75 m) was consistenly larger than the value predicted for that level from the six-point fit curves (i.e., using speeds obtained for $z < 6$ m). Thus, for example, in Figure 8*b* the observed speed at this level falls to the right of the dashed curve. However, if we assume the logarithmic layer extended to 19 m and do a seven-point fit to (1) (i.e., use the speed data for $z \leq$ 19 m), the computed r^2 is always larger than that necessary for a 0.99 confidence level for a seven-point according to the t test. Thus using this test one might conclude (we believe erroneously) that the speed profile was logarithmic up to 19 m.

By examining sample profiles we subjectively conclude that for a six-point fit when $r^2 \gtrsim 0.987$, the speed profile was logarithmic up z = 5.65 m. About 7% of the r^2 displayed in Figure 10*d* are less than 0.987. If we neglect the r^2 value determined from profiles obtained during the first 24 hours (see below), less than 2% were less than 0.987. In the sense that the r^2 values exhibit smooth behavior and are generally large (much greater than 0.84), and the inferred u_* and z_0 values also exhibit smooth behavior, an averaging time of 6 hours apparently yields reliable estimates of u_* and z_0.

During the first day of the experiment the current speeds are largest and the six-point fits are poorest (Figure 10). In other speed data from a similar instrument we have noticed that the measured profiles are relatively less logarithmic during the first few hours of observation. We suspect that the relatively poor fit for the first day's data in Figure 10 is not owing to the speeds being largest then but rather to an instrumental effect (e.g., grit in the motor bearings which gets washed out after a few hours).

One might expect a correlation between the current direction and r^2. For example, one might expect a better fit (larger r^2) when the flow was along the furrow axis and a worse fit (lower r^2) when the current direction was at an angle to the furrow. Figure 10*e* shows the current direction as a function of time measured concurrently by the VACM on the tripod instrument. Somewhat surprisingly there is little visual association in the r^2 and direction curves shown in Figure 10. Even a polar scatter plot of r^2 with current direction (not shown) shows no apparent pattern. This may be due to the fact that the current direction was rather constant 330° ± 25°.

While there is no apparent dependence of r^2 on current direction, r^2 values are found to be somewhat correlated with current speed. From Figure 11 one sees that scatter in r^2 decreases and the r^2 values themselves tend to be larger (better fit) with increasing current speed, neglecting those values (circled in this figure) from the first day's data. The reason for the improved fit (larger r^2) with higher current speed may be that relative to the integral time scale $\tau_i \approx z/U$, the averaging time T increases as the current speed increases since in the logarithmic layer $\overline{u^2}/U^2$ = constant. Somewhat better fits are to be expected as the averaging time T increases relative to the integral time scale τ_i (cf. (2)). This conclusion is reinforced when

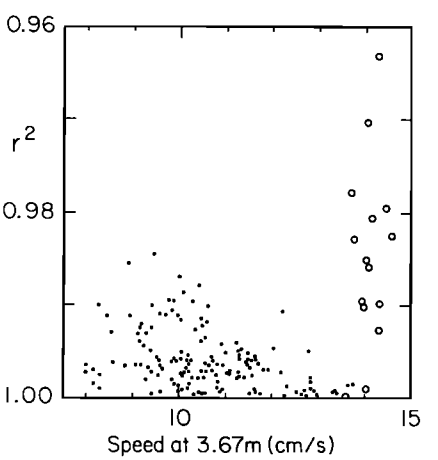

Fig. 11. Scatter plot of the r^2 values in Figure 8 and 6-hour averaged speed at 3.67 m. Circled values are those for the first day of the experiment.

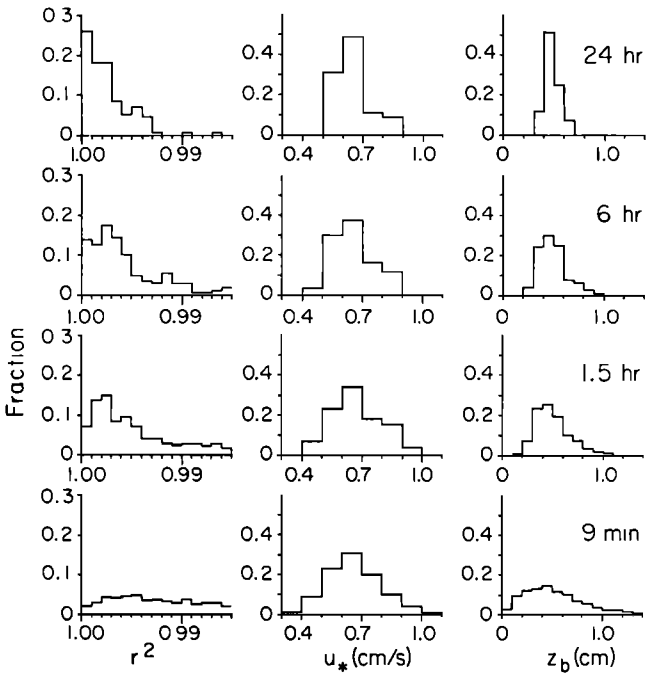

Fig. 12. Histograms of r^2, u_*, and z_0 values determined from six-point fits (going from top to bottom) of 24-hour, 6-hour, 1.5-hour, and 9-min averaged seeds to (1). Only the $r^2 > 0.985$ parts of the r^2 histograms are shown.

we later consider profiles formed from speeds averaged over times greater than and less than 6 hours.

Histograms of the u_* and z_0 values displayed in Figure 10 are provided in Figure 12. The peak value of u_* lies between 0.6 cm/s and 0.7 cm/s and that of z_0 somewhere between 0.4 cm and 0.5 cm. Mean values of u_* and z_0 estimated from consecutive 6-hour averaged profiles are the same as the values estimated from the mean profile (Figure 8), namely 0.66 cm/s and 0.49 cm, respectively.

The absolute heights of the lower rotors above the furrow floor are well known (Table 1) because of photographs taken of the instrument from the submersible *Trieste II*. To estimate the sensitivity of the inferred u_* and z_0 values to uncertainities in z, those values were recomputed by adding (subtracting) 5 cm to each rotor height. In histograms of these computed values, not presented here, the u_* peak increased (decreased) by about 15% (11%), and the z_0 peak increased (decreased) by about 60%(50%). According to histograms of the r^2 values, somewhat better fits occurred when 5 cm was added to each rotor height.

Histograms of r^2, u_*, and z_0 values determined from six-point fits (i.e., rotor 1–3 and 5–7 speeds as the input data) of 9 min, 1.5 hour, 6 hour, and 24 hour averaged data to (1) are presented in Figure 12. The poorest fits are obtained from the averaging interval of 9 min which is comparable to z/u_* (of the order of 10 min, Table 1). However, while the 9-min average fits are the worst, they still are not bad. Over 60% of these fits had $r^2 \geq 0.987$, and over 85% had $r^2 \geq 0.960$. For time scales of 9 min the flow profile is sufficiently logarithmic that reasonable estimates of u_* and z_0 can be obtained by using (1). Increasing the averaging intervals results in a smoothing of the u_* and the z_0 series. The histograms of u_* and z_0 in Figure 12 only become narrower as the averaging time increases. Consistently better fits (larger r^2) are obtained as the averaging interval is increased. For a stationary flow this is expected ((2)). However, for a nonstationary flow (i.e., in (1) $U = U(t)$) it is not apparent that this should be the case. The mean values of the u_*, the z_0, and the r^2 values inferred from consecutive 9 min, 1.5 hour, 6 hour, 24 hour, 256 h profiles are given in Table 2. The mean u_* value for the 24-hour averaged data is somewhat smaller than the others because the last 16 hours of data, when the current was relatively strong, does not contribute to this mean but does contribute to the others.

Implicit in the above is the assumption that the logarithmic layer extended to 5.65 m even when the current was relatively weak. If this were not the case one would expect relatively low r^2 values (poorer fits) for six-point fits to be associated with periods of weaker flow. A comparison of Figure 10*c* and 10*d* shows that this is not the case.

Earlier in discussing the speed spectrum for the record obtained at $z = 1$ m, the rise in the energy level occurring for $n \gtrsim 0.6$ cph was attributed to shear generated turbulent fluctuations in the BBL. If this is correct, then with $E(n)$ being the observed spectrum, $E_b(n)$ the estimated background spectrum, $n_1 = 0.6$ cmph and $n_2 = 3.33$ cph (the Nyquist frequency)

$$n_1 \int^{n_2} [E(n) - E_b(n)]\, dn \tag{3}$$

is the estimated contribution to $\overline{u^2}$ from BBL shear generated turbulent fluctuations with time scales $\geq 2x$ (sampling time) = 18 min. Applying (3) to the $z = 1$ m record gives 0.25 cm^2/s^2 as this estimated contribution to $\overline{u^2}$ is related to u_* by the relation

$$\overline{u^2} = 2.8\, u_*^2$$

according to *Mellor* [1973]. For $u_* = 0.66$ cm/s, this gives $\overline{u^2} = 1.2$ cm^2/s^2. Hence only about 20% of the variance in $\overline{u^2}$ associated with time scales ≥ 18 min.

g. *Sediment Erosion*

Shown as a time-lapse motion picture of the seabed, the film record from the tripod camera shows only one clear indication of hydrodynamic disturbance of the bottom. This is the washing away of one small ($\sim \frac{1}{2}$ cm) lump of sediment in the field of view of the camera at the beginning of the experiment. It is probably that this lump was a product of the disturbance caused by the apparatus landing on the seabed. Hence its erosion may not be significant, except that it suggests the likelihood of erosion of biogenic forms in the environment. After the tripod is moved to the furrow flank, no erosional activity is visible in the film. In particular, we see no perceptible migration of the three flank ripples in the field of view of the camera.

However, our measurements of u_* suggest that erosion may

TABLE 2. Average Over Consecutive Intervals of u_*, z_0, and r^2 Inferred From Six-Point Least Square Fits of (1) to Speeds Averaged Over Indicated Intervals

Averaging Interval	Number of Intervals	$\bar{u}_*$, cm/s	$\bar{z}_0$, cm	$\bar{r}^2$
255.6 hours (10.65 days)	1	0.663	0.49	0.9995
24 hours	10	0.654	0.47	0.9959
6 hours	42	0.662	0.49	0.9945
1.5 hours	170	0.663	0.50	0.9922
9 min	1704	0.662	0.56	0.9737

be occurring. The measurements of critical erosion stress summarized by *McCave* [1978] (Figure 8, recalculated from data of Southard and coworkers) show that material may be eroded by stresses as low as $u_* = 0.4$ cm/s. However, that is for calcareous ooze with high water content. The sediment of these furrows has 38–45% $CaCo_3$ and 52–58% water [*Flood*, 1978]. For calcareous ooze with this water content the critical erosion stress corresponds to $u_* \simeq 0.6$ cm/s. We conclude from our inferred u_* values that $u_* > 0.6$ cm/s about 68% of the time. If this critical $u_* = 0.6$ cm/s for erosion applies, then erosion of some of fine calcareous ooze presently occurs in the furrow floor. However, the presence of red clay which has a higher critical u_* for erosion ($u_* \gtrsim 3.5$ cm/s [*McCave*, 1978]) in the cohesive sediment at our site [*Flood*, 1978] may require a higher u_* than 0.6 cm/s erosion to occur. From shallow cores taken from the floor, the wall, and outside a small furrow in this region, *Flood* [1978] found the highest concentrations of coarse material in the core from the furrow floor and the lowest from the core outside the furrow. Also, the sedimentation rate was lowest on the furrow floor. Taken together, these observations indicate lesser deposition and perhaps selective removal of the fine material occurs at the furrow floor. The relative concentration of coarse material in the furrow floor was found to extend down to at least 40 cm, indicating a minimum age for the furrow of 11,000 years.

Another of *Flood*'s [1978] observations is that clumps of sargassum weed are commonly present on furrow floors but not in the interfurrow areas. In this region, after weed becomes waterlogged and sinks, it presumably moves freely across the sea floor until it is trapped by a furrow. It is likely that the presence of this debris in the furrow increases the local scouring action of the flow and thus helps maintain the furrow.

h. Temperature

Unlike the speed records the temperature records were less noisy clear to the bottom ($z < 6$ m). This is illustrated in Figure 13 in which a segment of the raw temperature records is shown. The records at $z = 0.90$, 1.35, and 5.77 m are essentially identical except for offsets; while that at $z = 29.7$ m is comparatively noisy. This is consistent with the lowest three thermistors being in the well-mixed layer and the fourth at 30 m generally being either in the 'thermocline,' which caps the mixed layer, or in the stably stratified water above the thermocline. Only when the current at 19 m attains a speed of about 20 cm/s does the noise level in the highest thermistor reduce to that of the other three thermistors. This suggests that at such times the mixed layer extends above $z = 30$ m. No conductivity, temperature, and depth or salinity, temperature, and depth casts were made during the time of the observations. However, a mixed layer of thickness ~30 m is not inconsistent with observations of these layers made at other times in the general area [*Flood*, 1978; *Greenwalt and Gordon*, 1978].

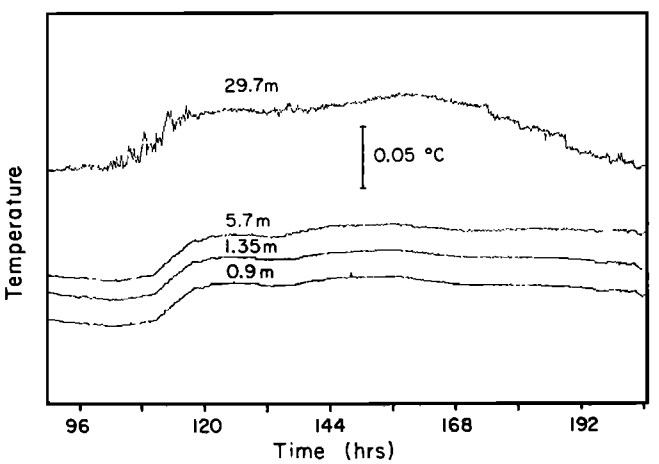

Fig. 13. Segment of the raw temperature time series measured by the four thermistors. For presentation purposes, some of the time series have been offset vertically by an arbitrary amount.

4. Discussion

The dozen days' data which we have obtained consists principally of current speeds above the bottom of a small furrow and simultaneous current speed and direction over the flank of a similar furrow. The most distinctive feature of these records is the steadiness of the current both in speed and in direction. Presumably because of this steadiness we find the logarithmic law fit to the data to be the best that we have seen for a benthic boundary layer (though at first we thought the furrow might prevent a log layer from forming). This logarithmic layer was characterized by friction velocity $u_* = 0.66$ cm/s, $z_0 = 0.5$ cm, and thickness $\delta_{in} \simeq 5.6$ m. The shear stress is larger than that determined for the BBL of the Florida Current ($u_* = 0.4$ cm/s) by *Weatherly* [1972]. From concurrent temperature records measured at four levels we infer the bottom mixed layer thickness $h_m \lesssim 30$ m.

Are the above values, $u_* \simeq 0.66$ cm/s, $z_0 \simeq 0.5$ cm, $\delta_{in} \simeq 5.6$ m, and $h_m \lesssim 30$ m, which are characteristic for the flow in and above the furrow, also plausible values for a bottom boundary layer formed over a nonfurrowed bottom? Below we attempt to show that they are. With $u_* = 0.66$ cm/s and $|\mathbf{V}_g| = 14.6$ cm/s, where $|\mathbf{V}_g|$ is the magnitude of the geostrophic current above the boundary layer taken to be the mean speed at 19 m, the geostrophic drag coefficient $C_d \equiv u_*/|\mathbf{V}_g| = 0.045$. This is not an unrealistic value for the inferred Rossby number $Ro = |\mathbf{V}_g|/fz_0 \simeq 5 \times 10^5$ [*Csanady*, 1967]. The value $z_0 = 0.5$ cm is too large to be a Nikuradse roughness parameter $\hat{z}_0$. For a smooth bottom $\hat{z}_0 \simeq 0.1\ \nu/u_*$ and for a rough bottom $\hat{z}_0 \simeq d/30$, where ν is the kinematic velocity and d is the height of the bottom roughness elements. With $\nu = 0.014$ cm^2/s and $u_* = 0.66$ cm/s, the former gives $\hat{z}_0 = 0.002$ cm. The latter expression with $\hat{z}_0 = 0.5$ cm requires roughness elements half the size of the lowest rotor in Figure 2. However, finding $z_0 \gg \hat{z}_0$ is not an uncommon occurrence in the bottom boundary layer [*Sternberg*, 1969; *Lesht*, 1978; *Wimbush and Lesht*, 1979]. *Businger and Arya* [1974] state that the thickness of the logarithmic layer $\delta_{in} \simeq (0.10 - 0.15)h$, where h is the thickness of the planetary boundary layer. Taking $h = 1.3\ u_*/[f\ (1 + N_0^2/f^2)^{1/4}]$ [*Weatherly and Martin*, 1978] with $u_* = 0.66 \times 10^{-2}$ m/s, $f = 0.692 \times 10^{-4}$ s^{-1}, $N_0 = 7 \times 10^{-4}$ s^{-1} this gives $\delta_{in} = (3.9 - 5.8)$m. Our inferred value falls in this range. Also, we have simulated this boundary layer by using the flat bottom model described in *Weatherly and Martin* [1978]. This is a one-dimensional model in which the boundary layer is assumed horizontally uniform. The input parameters to the model $|\mathbf{V}_g|$, f, z_0, and N_0 were assigned the values quoted above. The model predicted $u_* = 0.66$ cm/s, $\delta_{in} = 6$ m and $h_{mix} = 27$ m, which is in close agreement with values inferred from the data.

The data presented here are insufficient to determine whether the smaller furrows in the BBOR region are relic or active features. The presence of weed in the furrow may help

scour and maintain the furrows. The sharpness of corners at which the floor and walls meet suggests that these furrows are not just relic features.

The inferred u_* values for the furrow floor may be sufficiently large to result in erosion of some of the finer cohesive sediments. The results summarized in *McCave* [1978] suggest that calcareous ooze may be eroded for $u_* \gtrsim 0.6$ cm/s. This, together with the observation of coarsest sediments in the furrow bottom, less coarse in the furrow wall, and least coarse outside [*Flood*, 1978], leads us to speculate that the data are not inconsistent with these furrows being active features resulting from vortex rolls which cause the u_* values inside a furrow to be slightly larger than outside. The region of horizontal convergence near the surface is where the turbulence is largest [*Tennekes*, 1973] and should coincide with the furrow axes. If such vortex rolls do exist in this region of the BBOR, the reason for their existence (the postulated ubiquitous existance of such features in turbulent wall boundary layers [*Tennekes*, 1973] or Taylor-Goertler vortices associated with boundary layers on concave walls (see Figure 1 and *Schlichting* [1968, p. 504–509])) remains the subject for future work.

Acknowledgments. We thank all who contributed to the success of this experiment, especially E. Tankard, Jr. and D. Hunley, who developed the profiling instrument (Figures 2 and 3); L. Nemeth, who developed the tripod instrument (Figure 4); R. Harkema, who helped with the data analysis; the officers and crew of *Point Loma*, who deployed the instruments; and the officers and crew of *Trieste II*, who, with R. Flood, provided the in situ photographs (Figures 3 and 4), positioned the tripod instrument, and eventually rescued it when its release mechanism failed. Also, we are grateful to R. Flood, W. Grant, and I. McCave for their comments on an earlier manuscript. This research was sponsored by the Office of Naval Research under contracts N00014-78-C-0201 (G.W.) and N00014-76-C-0226 (M.W.) and the National Science Foundation under grant DES75-15688 (G.W.).

REFERENCES

Businger, J. A., and S. P. S. Arya, Height of the mixed layer in stably stratified planetary boundary layers, *Advan. Geophys., 18a*, 73–92, 1974.

Businger, J. A., J. C. Wyngaard, Y. Izumi, and E. F. Bradley, Flux profile relationships in the atmospheric surface layer, *J. Atmos. Sci., 28*, 181–189, 1971.

Csanady, G. T., On the resistance law of a turbulent Ekman layer, *J. Atmos. Sci., 24*, 467–471, 1967.

Flood, R. D., Studies of deep-sea sedimentary micro topagraphy in the North Atlantic Ocean, Ph.D. dissertation, Mass. Inst. of Tech., Cambridge, Mass., 1978.

Greenwalt, D., and C. M. Gordon, Short-term variability in the bottom boundary layer of the deep ocean, *J. Geophys. Res., 83*, 4713–4716, 1978.

Heezen, B. C., and C. D. Hollister, *The Face of the Deep*, 659 pp. Oxford University Press, New York, 1971.

Hollister, C. D., R. D. Flood, D. A. Johnson, P. F. Lounsdale, and J. B. Southard, Abyssal furrows and hyperbolic echo traces on the Bahama Outer Ridge, *Geology, 2*, 395–400, 1974.

Lesht, B. M., Field measurements of the bottom frictional Boundary layer in the New York Bight, Tech. Mem. *ERL MESA—28*, 167 pp, Nat. Oceanic and Atmos. Admin., Boulder, Colo, 1978.

McCave, I. N., Sediments in the abyssal boundary layer, *Oceanus, 21*, 27–33, 1978.

McCullogh, J. R., Vector averaging current meter speed calibration and recording technique, *Tech. Rep. 75-44*, 35 pp., Woods Hole Oceanogr. Inst., Woods Hole, Mass., 1975.

Mellor, G. L., Analytic prediction of properties of stratified planetary surface layers, *J. Atmos. Sci., 30*, 1061–1069, 1973.

Monin, A. S., The atmosphere boundary layer, in *Annual Reviews of Fluid Mechanics*, vol. 2, pp. 225–250, Annual Reviews, Palo Alto, Calif., 1970.

Schlichtning, H., *Boundary Layer Theory*, 748 pp., McGraw-Hill, New York, 1968.

Smith, J. D., and S. R. McLean, Boundary layer adjustments to bottom topography and suspended sediment, in *Bottom Turbulence*, pp. 123–152, Elsevier, New York, 1977.

Sternberg, R. W., Field measurements of the hydrodynamic roughness of the deep sea boundary, *Deep Sea Res., 19*, 413–420, 1969.

Tenneckes, H., Similarity laws and scale relations in planetary boundary layers, in *Workshop on Micro-meteorology*, edited by D. A. Haugen, pp. 177–216, American Meteorological Society, Boston, Mass., 1973.

Tenneckes, H., and J. L. Lumley, *A First Course in Turbulence*, 300 pp., MIT Press, Cambridge, Mass., 1972.

Weatherly, G. L., A study of the bottom boundary layer of the Florida current, *J. Phys. Oceanogr., 2*, 54–72, 1972.

Weatherly, G. L., and P. J. Martin, On the structure and dynamics of the oceanic bottom boundary layer, *J. Phys. Oceanogr., 8*, 557–570, 1978.

Weatherly, G. L., and J. C. Van Leer, On the importance of stable stratification to the structure of the bottom boundary layer on the western Florida shelf, in *Bottom Turbulence*, pp. 103–122, Elsevier, New York, 1977.

Wimbush, M., and B. M. Lesht, Current induced sediment movement in the deep Florida Straits: Critical parameters, *J. Geophy. Res., 84*, 2495–2502, 1979.

Wimbush, M., and W. Munk, The benthic boundary layer, in *The Sea*, vol. 4, part 1, pp. 731–758, John Wiley, New York, 1970.

Wyngaard, J. C., On surface layer turbulence, *Workshop on Micrometeorology*, edited by D. A. Haugen, pp. 101–149, American Meterology Society, Boston, Mass., 1973.

Yalin, M. S., *Mechanics of Sediment Transport*, 298 pp., Pergamon, New York, 1977.

(Received July 3, 1979;
revised January 3, 1980;
accepted February 21, 1980.)